Spectral evolution with doping of an antiferromagnetic Mott state

Huan-Kuang Wu[1,2] and Ting-Kuo Lee[1]
[1]*Institute of Physics, Academia Sinica, Nankang Taipei 11529, Taiwan*
[2]*Department of Physics, National Taiwan University, Daan Taipei 10617, Taiwan*
(Received 26 August 2015; revised manuscript received 4 December 2016; published 20 January 2017)

Since the discovery of half-filled cuprate to be a Mott insulator, the excitation spectra above the chemical potential for the unoccupied states has attracted much research attention. There were many theoretical works using different numerical techniques to study this problem, but many have reached different conclusions. One of the reasons is the lack of very detailed high-resolution experimental results for the theories to be compared with. Recently, the scanning tunneling spectroscopy [P. Cai *et al.*, Nat. Phys. **12**, 1047 (2016); C. Ye *et al.*, Nat. Commun. **4**, 1365 (2013)] on lightly doped Mott insulator with an antiferromagnetic order found the presence of in-gap states with energy of order half an eV above the chemical potential. The measured spectral properties with doping are not quite consistent with earlier theoretical works. Although the experiment has disorder and localization effect, but for the energy scale we will study here, a model without disorder is sufficed to illustrate the underlying physics. We perform a diagonalization method on top of the variational Monte Carlo calculation to study the evolution of antiferromagnetic Mott state with doped hole concentration in the Hubbard model. Our results found in-gap states that behave similarly with ones reported by STS. These in-gap states acquire a substantial amount of dynamical spectral weight transferred from the upper Hubbard band. The in-gap states move toward chemical potential with increasing spectral weight as doping increases. Our result also provides information about the energy scale of these in-gap states in relation with the Coulomb coupling strength U.

DOI: 10.1103/PhysRevB.95.035133

I. INTRODUCTION

The spectral properties of the Mott insulators as a function of doping has been one of the key issues in studying the physics of high-T_c cuprate superconductors. There are many theoretical works on this topic including exact diagonalization (ED) [1–3], quantum Monte Carlo (QMC) [4] method, dynamical cluster approximation (DCA) [5], dynamical mean field theory (DMFT) and cluster-DMFT [6–10], and also real-space Green's function approach [11]. According to their results, generally, a clear spectral weight transferred from the upper Hubbard band (UHB) to lower Hubbard band (LHB) that situated at the chemical potential can be seen as doping increases. However, the details are different. There are in-gap signals found in many works. In Refs. [2,5,6], these signals become farther away from chemical potential together with the UHB as doping increases. Similarly, in Ref. [7], there are two peaks near Fermi energy that also move away from each other as doping increases. On the other hand, in several cluster-DMFT works [8,9], the in-gap signals move toward the chemical potential as doping increases. In Ref. [8] the in-gap signal exists at half-filling in paramagnetic or antiferromagnetic (AFM) states. There were also several results reported by using the cluster perturbation theory (CPT). For the electron-doped case [12], an in-gap state was found at the lower edge of UHB, which is in agreement with the in-gap states seen by STS on $Ca_2CuO_2Cl_2$ [13] near an impurity. For the hole-doped case [14–18], there were low-energy in-gap states with energy less than $0.2U$. On the experimental side, the x-ray absorption spectra (XAS) [19,20] have observed the spectral weight transferred from UHB to LHB as doping increases but the broadness of the peaks makes it difficult to make a detailed comparison.

Recently, STS [13,21] reported for very underdoped cuprates with a long range AFM order probed the spectral function across the charge-transfer (CT) gap. It found some new results unexpected from earlier theoretical works. In Ref. [21], finite density of states appears inside and throughout the CT gap and only a small energy range at the chemical potential remains empty of spectral weight after holes are doped into the sample. This small gap seems to be related to the disorder that causes localization of the states near chemical potential. On the other hand, those in-gap states at lower doping can be high above chemical potential reaching up to 40% of CT gap. This is much larger than the in-gap states reported earlier [9,12,14–18] for HM calculations with U representing the CT gap. Besides the presence of in-gap states, when the system is doped with holes, there is also a systematic evolution in the spectral weight distribution or local density of states (LDOS) measured at different positions. The in-gap states with larger spectral weight are situated closer to the chemical potential, while at the same time the spectral weight of UHB moves to higher energy. This relation is opposite to that found in earlier works [2,5,6], where in-gap peak moves to higher energy as doping increases. Finally, the positions are anticorrelated between sites with higher spectral weight for UHB and in-gap states. This is consistent with an effective doping picture. That is, at the position where the UHB has strong intensity, the effective doping is close to zero or no doping and the in-gap states are not seen. On the other hand, at the position where the in-gap states show up, doping is finite and the intensity of the UHB becomes weaker. Note that similar results have been found previously in optical conductivity measurements [22–24], where there are also peaks around the scale of half an eV at low doping which moves to the lower energy as hole concentration increases. The discrepancy between this newly measured weight distribution and its doping dependence with earlier theoretical works has motivated us to examine the theoretical prediction again and more carefully.

In this work we study the spectral evolution of Mott state with hole doping by a variational approach but with explicit presence of the AFM long range order as in the experiment [13]. We are particularly interested in the spectra of the unoccupied states above the chemical potential. In the strong coupling regime ($U \geqslant 8t$), at half-filling or in the parent compound, each site is already occupied by an electron with spin 1/2. Hence, when an electron is inserted into the half-filled state, it must create a doubly occupied site (doublon) with final states in the UHB and there are no states inside the CT gap. However, after hole doping, when an electron is inserted into the lattice, there are two possible final states. The original LHB splits into upper and lower spin density wave (SDW) bands in the presence of AFM order. In this case, finite in-gap spectral weight that corresponds to the upper SDW states shows up. These states, according to our calculation, behave in a similar manner to the in-gap states recently found by STS [13,21] with respect to the energy scale and evolution. Although the experiment exhibits disorder and localization effect, here we only consider the simple case without disorder but it already catches the main behavior.

These in-gap states also have components of states in the UHB with doublons despite the main contribution from upper SDW states. Thus these in-gap states are a mixture of upper SDW and UHB states and they absorb most of the spectral weight transferred from UHB. As hole doping increases, in-gap states move toward the chemical potential with increasing spectral weights and the energy separation between UHB and LHB is effectively getting smaller. This provides a slightly different version from the ED result [1] without including the AFM order, which shows that the weights are transferred from UHB to LHB as the holes are doped but the band-edge separation has little dependence on the hole concentration.

Below we first calculate the ground state of a one-band Hubbard model (HM) in the presence of the AFM order by means of the variational Monte Carlo (VMC) method. Then several states with one electron added to the ground state are proposed. These states contributing to the unoccupied states or the inverse photoemission spectra (IPES) are orthogonalized to find the quasiparticle states. Then the spectral weights of these states are all calculated and compared with experiment [13,21] with respect to the energy evolution and the spectral weight redistribution. In addition, we also examine our results for different values of U to study the changes from weak to strong coupling.

II. FORMALISM AND METHOD

A well-known model which includes the low energy physics in CuO_2 planes is the three-band HM [25]. In this model, the parent compound without any extra doped holes has every Cu in $3d^9$ configuration with a spin 1/2 hole. This is like a half-filled one-band HM with very large on-site Coulomb repulsion U and every site has a spin 1/2. When a hole is doped into the CuO_2 plane, it resides at the oxygen site [26]. Due to the strong superexchange interaction between the Cu spin and the doped hole on oxygen, Zhang and Rice [27] found the interaction of two oxygen p orbitals and Cu d orbital leading to three bands, the nonbonding states, antibonding triplet states, and the bonding singlet states known as the Zhang-Rice (ZR) singlet. There are large energy differences between the three states and only ZR singlet is assumed to be important for consideration. This ZR singlet in the three-bands model is similar to the vacant site when the hole is doped into the one-band HM. When the energy difference between ZR singlet and the Cu $3d^{10}$ state, which is the effective CT gap, is not punitively large, the Cu hole can jump to its neighboring oxygen to form ZR singlet while the original Cu turns into a $3d^{10}$ configuration without spin. This is similar to the charge fluctuation process in one-band HM to turn the two nearest neighbor opposite spins into the short lived configuration of a doublon-hole pair. By making the correspondences of the doublon in one-band HM with the Cu $3d^{10}$, the Hubbard gap with the CT gap, and the vacant site or hole with the ZR singlet, we could clarify the physics by studying the one-band HM instead of the more complicated three-band model [28,29].

The one-band HM we consider is

$$H = -t \sum_{\langle i,j\rangle,\sigma} (c^{\dagger}_{i,\sigma} c_{j,\sigma} + \text{H.c.}) + \sum_{i} U n_{i,\uparrow} n_{i,\downarrow}, \qquad (1)$$

where t is the hopping integral of a single electron and $\langle i,j\rangle$ denotes the nearest-neighbor sites. U/t is the on-site repulsion which will be taken to be 10 in the present work unless otherwise specified.

The variational ground state we choose in the VMC method is the Jastrow type state with coexisting antiferromagnetism and d-wave superconductivity [30,31]:

$$|\Psi_{\text{variational}}\rangle \equiv \hat{P}_{d-h} \hat{P}_{d} |\Psi_{afm-ds}\rangle, \qquad (2)$$

where $\hat{P}_d = g^{\hat{d}}$ is the Gutzwiller projection operator with $\hat{d} = \sum_i \hat{d}_i = \sum_i \hat{n}_{i\uparrow}\hat{n}_{i\downarrow}$ representing the doublon number. The Gutzwiller factor g suppresses the double occupancy or doublon number when it is less than one. The Jastrow factor for doublon-hole binding [32] is $\hat{P}_{d-h} \equiv \prod_i [1 - Q_{d-h}\hat{d}_i \prod_\tau (1 - \hat{h}_{i+\tau})]$, where τ connects the nearest neighbors and $\hat{h}_i \equiv (1-\hat{n}_{i\uparrow})(1-\hat{n}_{i\downarrow})$ is the number of holes on site i. This factor ensures the insulating phase at half filling. Such factor may come in different forms. Here we restricted the occurrence of free doublons that aren't bound with holons with a variational parameter $Q_{d-h} \leqslant 1$. The wave function $|\Psi_{afm-ds}\rangle$ with coexisting antiferromagnetism and superconductivity has been proposed before [30],

$$|\Psi_{afm-ds}\rangle \equiv \hat{P}^{Ne} \prod_{k\in MBZ} (u_{k-} + v_{k-}\alpha^{\dagger}_{k\uparrow}\alpha^{\dagger}_{k\downarrow}) \times (u_{k+} + v_{k+}\beta^{\dagger}_{k\uparrow}\beta^{\dagger}_{-k\downarrow})|0\rangle, \qquad (3)$$

where $\hat{P}^{Ne}$ restricts the state to have Ne electrons. The operators

$$\alpha^{\dagger}_{k\sigma} \equiv a_k c^{\dagger}_{k,\sigma} + \sigma b_k c^{\dagger}_{k+Q,\sigma},$$
$$\beta^{\dagger}_{k\sigma} \equiv -\sigma b_k c^{\dagger}_{k,\sigma} + a_k c^{\dagger}_{k+Q,\sigma} \qquad (4)$$

correspond to the lower (α) and upper (β) spin density wave states with coefficients $a_k^2 \equiv \frac{1}{2}(1 - \frac{\varepsilon_k}{\sqrt{\varepsilon_k^2 + M_v^2}}), b_k^2 \equiv 1 - a_k^2$, M_v being a variational parameter proportional to staggered magnetization. Here we consider commensurate SDW and Q is chosen to be (π,π), and k is within the magnetic Brillouin zone (MBZ). The coherent coefficients $u_{k\pm}$ and $v_{k\pm}$ are defined by $u^2_{k\pm} \equiv \frac{1}{2}(1 - \frac{(E_{k\pm}-\mu)}{\sqrt{\Delta_k^2 + (E_{k\pm}-\mu)^2}})$ and $v^2_{k\pm} \equiv 1 - u^2_{k\pm}$,

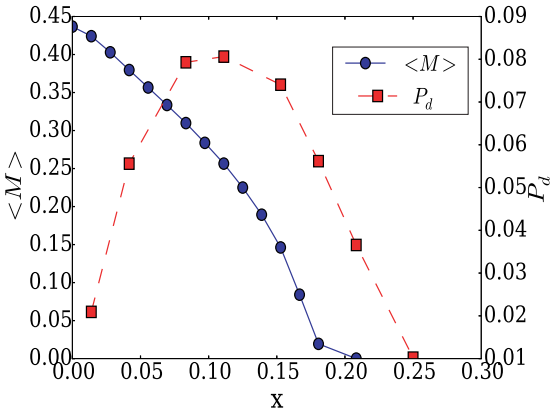

FIG. 1. Ground state staggered magnetization $\langle M\rangle$ and coexisting long range pair-pair correlation function P_d as a function of hole concentration for $U = 10t$ in a 12×12 lattice. The AFM order disappears around 0.18 doping in this model.

respectively. The plus/minus sign denotes upper/lower SDW states; $E_{k\pm} \equiv \pm\sqrt{M_v^2 + \varepsilon_k^2}$ is the mean field SDW energy with $\varepsilon_k \equiv -2t(\cos k_x + \cos k_y)$. The chemical potential μ is also taken to be a variational parameter. Finally, $\Delta_k = \Delta(\cos k_x - \cos k_y)$ is the d-wave gap. For numerical convenience, our boundary condition is chosen to be periodic in x direction and antiperiodic in y direction.

Figure 1 shows the ground state staggered magnetization $\langle M\rangle = \frac{1}{N_s}\Sigma_i e^{iQ\cdot R_i}\langle S_{iz}\rangle$, where N_s denotes number of sites, and the long range pair-pair correlation $P_d \equiv P_d(R = (L/2, L/2)) = \Sigma_i \Sigma_{\alpha,\alpha'} \lambda_{\alpha,\alpha'} \langle \Delta^\dagger_{i+R,\alpha} \Delta_{i,\alpha'}\rangle / N_s$, where $\Delta_{i,\alpha} = \frac{1}{\sqrt{2}}(c_{i\uparrow}c_{i+\hat{\alpha}\downarrow} - c_{i\downarrow}c_{i+\hat{\alpha}\uparrow})$, $\hat{\alpha} = \pm\hat{x}$ or $\pm\hat{y}$, and $\lambda_{\alpha,\alpha'} = 1$ if α and α' are in the same axis and $\lambda_{\alpha,\alpha'} = -1$ otherwise. The result that AFM order disappears around 18% as well as the value of coexisting P_d agrees with Ref. [31] even though they have used a more sophisticated trial wave function [33]. Since the trial wave function we used has pairing in it, there is coexistence of superconductivity and antiferromagnetism as seen in Ref. [31]. This issue will be discussed further in the conclusion.

By adding an electron to the ground state we can now calculate the IPES. We shall consider the simplest quasiparticle states and there are four kinds for each k point within the MBZ:

$$|1_{k,\sigma}\rangle \equiv \sum_i \hat{n}_{i,\bar{\sigma}}(e^{ik\cdot R_i} c^\dagger_{i,\sigma})|g_N\rangle, \tag{5}$$

$$|2_{k,\sigma}\rangle \equiv \sum_i \hat{n}_{i,\bar{\sigma}}(e^{i(k+Q)\cdot R_i} c^\dagger_{i,\sigma})|g_N\rangle, \tag{6}$$

$$|3_{k,\sigma}\rangle \equiv \sum_i \left\{(1-\hat{n}_{i,\bar{\sigma}})\prod_\tau \left[1 - \hat{d}_{i+\tau}\prod_{\rho\neq-\tau}(1-\hat{h}_{i+\tau+\rho})\right] \times (e^{ik\cdot R_i} c^\dagger_{i,\sigma})\right\}|g_N\rangle, \tag{7}$$

$$|4_{k,\sigma}\rangle \equiv \sum_i \left\{(1-\hat{n}_{i,\bar{\sigma}})\prod_\tau \left[1 - \hat{d}_{i+\tau}\prod_{\rho\neq-\tau}(1-\hat{h}_{i+\tau+\rho})\right] \times (e^{i(k+Q)\cdot R_i} c^\dagger_{i,\sigma})\right\}|g_N\rangle, \tag{8}$$

where ρ and τ connect nearest neighbors and $|g_N\rangle$ denotes the variational ground state we found with N electrons. States $|1\rangle$ and $|2\rangle$ both create an extra doublon in the ground state, so they belong to the UHB in the atomic limit. On the contrary, states $|3\rangle$ and $|4\rangle$ add an electron to a vacant site, and they belong to the LHB. Note that at low hole concentration, there are finite doublon-hole bound pairs generated by quantum fluctuation. If we add an electron to the hole site bound with a doublon, it would create a free doublon. these states are also in the UHB, which we had confirmed by direct calculation of their energy. These states have large overlaps with $|1\rangle$ and $|2\rangle$ and they also contribute very little spectral weight which is proportional to the doublon number. So without loss of generality we shall exclude the process of creating free doublon from states $|3\rangle$ and $|4\rangle$.

To find the eigenstates within the chosen basis, for each k point in MBZ, we calculated the Hamiltonian matrix element by Monte Carlo algorithm $\langle H(k,\sigma)\rangle_{ij} = \langle i_{k,\sigma}|H|j_{k,\sigma}\rangle$ $(i,j = 1\text{–}4)$. Since it is a nonorthonormal basis, we also need the metric tensor, $\langle G(k,\sigma)\rangle_{ij} = \langle i_{k,\sigma}|j_{k,\sigma}\rangle$. Next, we solve the 4×4 generalized eigenvalue problem and obtain four eigenstates with one quasiparticle added to the ground states which are denoted by the wave functions $|\Psi^i_{N+1}(k,\sigma)\rangle$ $(i = 1\text{–}4)$ with total energy $E^i_{N+1}(k,\sigma)$. The energy to insert a quasiparticle is defined as

$$\xi^{i+}(k,\sigma) = E^i_{N+1}(k,\sigma) - E_{N+1,\,\min}, \tag{9}$$

where the minimum eigenenergy, $E_{N+1,\,\min} \equiv \min\{E^i_{N+1}(k,\sigma)|i,k\}$, is considered to be at the chemical potential.

The spectral weight of inserting a particle of momentum k to the ground state contains two contributions $Z^+(k,\sigma)$ and $Z^+_Q(k,\sigma)$, which are defined by

$$Z^{i+}(k,\sigma) = \left|\langle\Psi^i_{N+1}(k,\sigma)|c^\dagger_{k,\sigma}|g_N\rangle\right|^2, \tag{10}$$

$$Z^{i+}_Q(k,\sigma) = \left|\langle\Psi^i_{N+1}(k,\sigma)|c^\dagger_{k+Q,\sigma}|g_N\rangle\right|^2. \tag{11}$$

A similar procedure is also applied to study states with an electron removed from the ground state; this is for the photoemission spectra (PES). The states can be simply obtained by a transformation $c^\dagger \to c$. The basis states are

$$|1^-_{k,\sigma}\rangle \equiv \sum_i \hat{n}_{i,\sigma}(e^{-ik\cdot R_i} c_{i,\bar{\sigma}})|g_N\rangle, \tag{12}$$

$$|2^-_{k,\sigma}\rangle \equiv \sum_i \hat{n}_{i,\sigma}(e^{i(-(k+Q)\cdot R_i)} c_{i,\bar{\sigma}})|g_N\rangle, \tag{13}$$

$$|3^-_{k,\sigma}\rangle \equiv \sum_i \left\{(1-\hat{n}_{i,\sigma})\prod_\tau \left[1 - \hat{d}_{i+\tau}\prod_{\rho\neq-\tau}(1-\hat{h}_{i+\tau+\rho})\right] \times (e^{-ik\cdot R_i} c_{i,\bar{\sigma}})\right\}|g_N\rangle, \tag{14}$$

$$|4^-_{k,\sigma}\rangle \equiv \sum_i \left\{(1-\hat{n}_{i,\sigma})\prod_\tau \left[1 - \hat{d}_{i+\tau}\prod_{\rho\neq-\tau}(1-\hat{h}_{i+\tau+\rho})\right] \times (e^{-i(k+Q)\cdot R_i)} c_{i,\bar{\sigma}})\right\}|g_N\rangle. \tag{15}$$

After diagonalization we have four eigenstates with a particle removed $|\Psi^{i-}_{N-1}(k,\sigma)\rangle$ ($i = 1$–4) from the ground state and their corresponding energies are $E^{i-}_{N-1}(k,\sigma)$ for each k. The energy to remove a particle becomes

$$\xi^{i-}(k,\sigma) = -E^{i}_{N-1}(k,\sigma) + E_{N-1,\,\mathrm{min}}. \tag{16}$$

Similarly, the minimum eigenenergy $E_{N-1,\,\mathrm{min}} \equiv \min\{E^{i}_{N-1}(k,\sigma)|i,k\}$ is considered to be at the chemical potential. The spectral weights to remove a particle are related to $Z^{-}(k,\sigma)$ and $Z^{-}_{Q}(k,\sigma)$ defined by

$$Z^{i-}(k,\sigma) = \left|\langle\Psi^{i}_{N-1}(k,\sigma)|c_{-k,\sigma}|g_N\rangle\right|^2, \tag{17}$$

$$Z^{i-}_{Q}(k,\sigma) = \left|\langle\Psi^{i}_{N-1}(k,\sigma)|c_{-k+Q,\sigma}|g_N\rangle\right|^2. \tag{18}$$

Finally we combine the PES and IPES together. Due to the finite size effect, we employed Lorentzian broadening $L(x;x_0,\Gamma) = \frac{1}{\pi}\frac{\Gamma/2}{(x-x_0)^2+(\Gamma/2)^2}$ with $\Gamma = 0.15t$ for the delta functions corresponding to each of the eigenstates:

$$\rho(\omega) = \frac{1}{N_s}\sum_{i,k,\sigma}\Big[\big(Z^{i+}(k,\sigma) + Z^{i+}_{Q}(k,\sigma)\big)L(\omega;\xi^{i+}(k,\sigma),0.15t) + \big(Z^{i-}(k,\sigma) + Z^{i-}_{Q}(k,\sigma)\big)L(\omega;\xi^{i-}(k,\sigma),0.15t)\Big]. \tag{19}$$

The summation is over i, k, and σ. Results reported here are mainly carried out on a 12×12 lattice.

III. RESULTS

The spectral function for $U/t = 10$ is plotted as a function of energy for three hole concentrations in Fig. 2. A sharp UHB peak around $9t$ is seen. More importantly, a broad band of in-gap states appears in the range $0.1U$–$0.35U$ which we believed to be mostly unoccupied upper SDW states. These states are about the same energy range as the newly found signals in the STS [13,21] if we consider U as the CT gap energy about 1.7 eV. As hole concentration increases, the UHB weight shifts toward higher energy while the in-gap states moves toward the chemical potential, i.e., the energies of in-gap states decrease. The spectral weights of these in-gap states also increase with doping. There is clearly a spectral weight transferred from UHB to low energy states (LES) that are between chemical potential and UHB. In Fig. 3, we compare the spectra obtained with three sizes of lattice. It is in good agreement with Fig. 2 that the peak positions of the in-gap states decrease with increased spectral weight, while UHB peaks move toward higher energies with reduced spectral weight as hole concentration increases. Note that since the chosen broadening parameter $\Gamma = 0.15t$ is larger than the SC energy scale, the linear density of states near chemical potential from d-wave superconductivity is not visible in the spectral function.

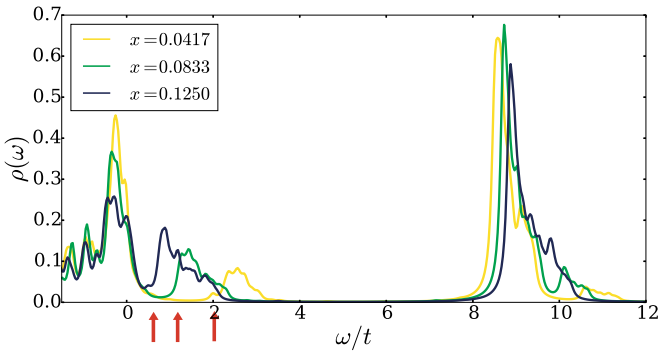

FIG. 2. Spectral function for doping $x = 0.0417$, 0.0833, and 0.125. $\omega = 0$ corresponds to the chemical potential. A Lorentzian broadening with width $\Gamma = 0.15t$ is applied to the delta functions for the eigenstates. The arrows indicate the value of ξ_0 as defined in the text.

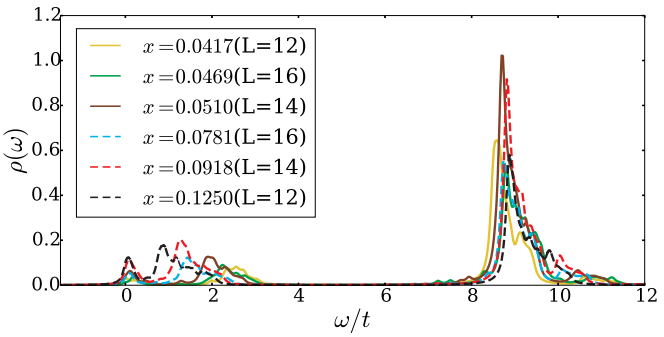

FIG. 3. IPES for several doping in different system size with $L = 12$, 14, and 16. The systematic evolution of the spectra with doping is preserved for different lattice sizes.

To verify the relationship between in-gap states and the upper SDW states, we calculate the inner product between these states. The upper SDW states can be constructed in the same way as wave functions $|3\rangle$ and $|4\rangle$ except now we restrict the electron to be inserted into the upper SDW band defined in Eq. (4),

$$|\psi_{u-SDW}(k,\sigma)\rangle \equiv \sum_i \left\{(1-\hat{n}_{i,\bar{\sigma}})\prod_\tau\left[1-\hat{d}_{i+\tau}\prod_{\tau\neq-\tau}(1-\hat{h}_{i+\tau+\tau})\right] \times (\beta_{k,\sigma}(i)c^{\dagger}_{i,\sigma})\right\}|g_N\rangle, \tag{20}$$

where $\beta_{k,\sigma}(i) = -\sigma b_k e^{ik\cdot R_i} + a_k e^{i(k+Q)\cdot R_i}$ is the coefficient of the upper SDW state, with momentum k and spin σ, at site i. At each of the k points, we found large overlap (> 0.8) between $|\psi_{u-SDW}(k,\sigma)\rangle$ and the in-gap states. Thus these in-gap states are essentially the upper SDW states although there are contributions from states $|1_{k,\sigma}\rangle$ and $|2_{k,\sigma}\rangle$ which are in the UHB. Besides these states near the chemical potential, there are also contributions from lower SDW states that are now vacant due to hole doping. The energy scale of these states is roughly determined by the coupling between the states $|3_{k,\sigma}\rangle$ and $|4_{k,\sigma}\rangle$. Considering the transition between upper and lower SDW states, our result gives a possible explanation of the half an eV peak in optical conductivity measurements [22–24] that shows a decreasing absorption energy and an increasing weight with more doping. This will be left for future works.

In the presence of AFM long range order, staggered magnetization opens a gap between the upper and lower SDW states. In our case, the effective staggered magnetization is proportional to the variational magnetic field M_v. To

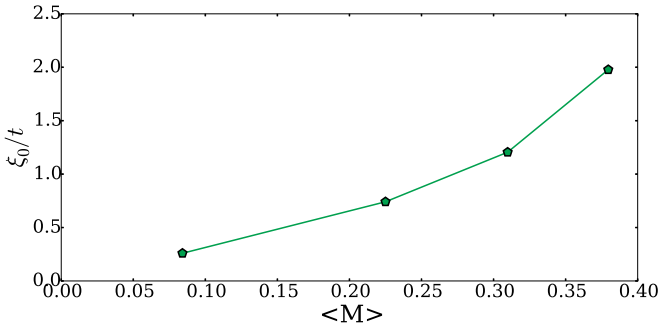

FIG. 4. ξ_0 of the upper SDW states as a function of magnetization. The energy together with magnetization are collected from four different doping $x = 0.0417$, 0.0833, 0.125, and 0.1667; here magnetization is inversely proportional to hole concentration.

illustrate this relation, we define ξ_0 by the lowest eigenenergy of the quasiparticle states that has an inner product with $|\psi_{u-SDW}(k,\sigma)\rangle$ larger than 0.8 [34], which provides a good indicator of the lower edge of the in-gap states. Thus positive correlation is expected between the upper SDW band edge ξ_0 and AFM strength $\langle M\rangle$ as shown in Fig. 4. Since $\langle M\rangle$ is inversely correlated with doping, this gives a natural explanation of the reduction of energies of in-gap states as doping increases. Next we shall examine the spectral weight transferred from UHB to LES. We calculated the total weight W_{UHB} and W_{LES}:

$$W_{UHB} \equiv \int_{4t}^{\infty} \rho(\omega)d\omega,$$
$$W_{LHB} \equiv \int_{0}^{4t} \rho(\omega)d\omega = 1 + x - W_{UHB}. \qquad (21)$$

W_{UHB} and W_{LES} at different doping are shown in Fig. 5. This agrees quantitatively with the previous results from ED [1], ED + cluster-DMFT [35], and CPT [17] despite the fact that AFM order was not considered in these works. This shows that the appearance of AFM order doesn't affect total spectral weight transferred as the sum rule should be satisfied.

If we consider each site at the atomic limit, UHB is completely unoccupied at half filling hence it has a spectral weight equal to 1. This weight W_{UHB} reduces to $1 - x$ when x holes are doped into the system. Upon doping, an electron

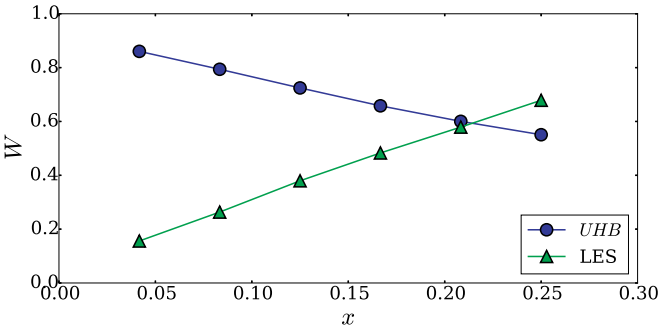

FIG. 5. Total spectral weight for UHB and LES. In under-doped regime, W_{UHB} and W_{LES} evolve linearly. By fitting, we found the slope to be -1.66 for W_{UHB} and 2.69 for W_{LES}.

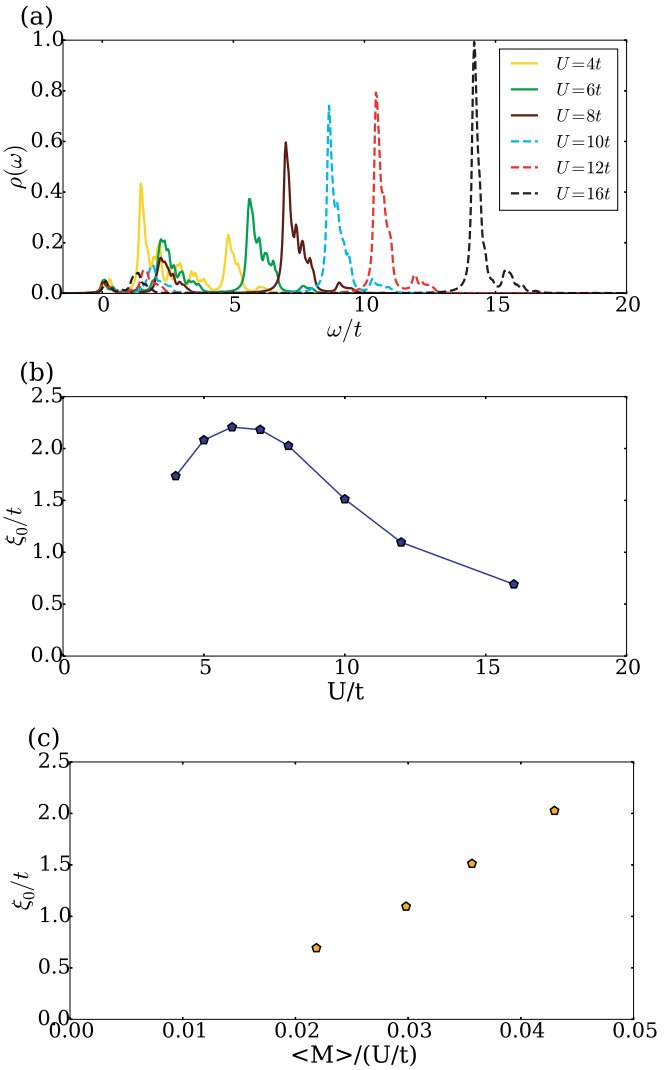

FIG. 6. (a) IPES for different U at $x = 0.0556$. (b) ξ_0/t at different U. (c) ξ_0/t as a function of $\langle M\rangle/(U/t)$ for $U \geqslant 8t$. This shows that the virtual exchange interaction J accounts for the results.

could be added to the empty or hole site in two choices from the spin degrees of freedom; hence the spectral weight for W_{LES} is $2x$. However, it is known that beyond this atomic limit there should be a dynamical correction [36] that comes from the coupling between these states which enhances the weight transfer and would give $W_{UHB} = 1 - x - \alpha$ and $W_{LES} = 2x + \alpha$. According to our calculation, the renormalization α at $U/t = 10$ is around $0.65x$.

Since the AFM order depends on U, it is important to examine the evolution of spectral functions with different values of U. In Fig. 6(a), the spectral functions for inserting a quasiparticle in the ground state are plotted for a range of U values. For $U/t \geqslant 6$, the separation between UHB and LES is clear and, as expected, UHB energy scales with U. The trend suggests that as U becomes smaller, weight of in-gap state at $x = 0.0556$ becomes larger and their component of $|1\rangle$ and $|2\rangle$ increases. For weak or intermediate U/t the weight of the in-gap state is comparable or even larger than that of UHB. To further examine the U dependence of these spectra, we plot

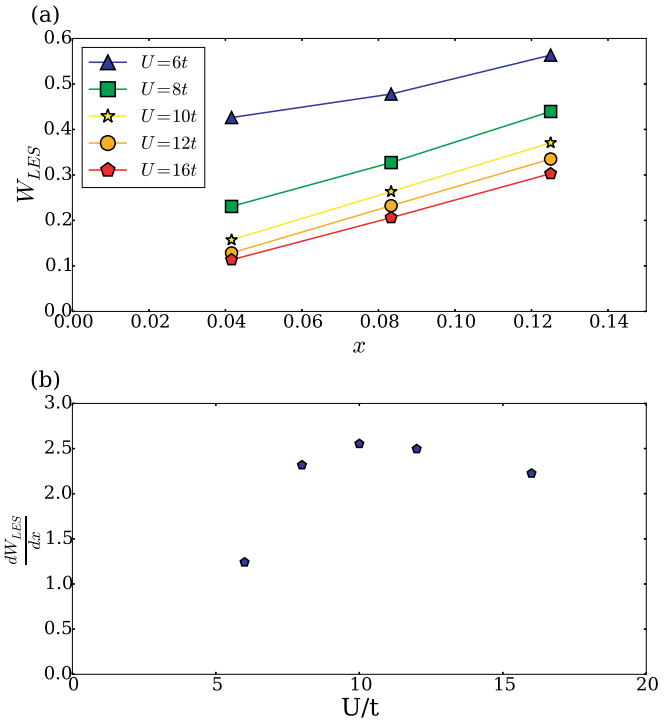

FIG. 7. (a) W_{LES} for different U at $x = 0.0417$, 0.0833, and 0.125. (b) Slope of W_{LES} for different U determined by the differences at $x = 0.0417$ and $x = 0.0833$.

the upper SDW band edge ξ_0 as a function of U in Fig. 6(b). Before U reaches $U_c \sim 8t$ to enter the Mott region, the ξ_0 is proportional to U/t. This is expected from a mean-field treatment for a weak or intermediate coupling U in the one-band HM, as the gap due to AFM order is proportional to $\langle M\rangle U$. Once the system enters the Mott region with U greater than U_c, it is the superexchange interaction J that determines the AFM order. Hence $\xi_0 \sim \langle M\rangle J \sim \langle M\rangle/(U/t)$. ξ_0 is plotted as a function of $\langle M\rangle/(U/t)$ in Fig. 6(c) for $U \geqslant U_c$. This shows that one could expect a maximum energy for in-gap states when U/t is near the critical value for a Mott transition.

Now let us examine the spectral weight for LES. As shown in Fig. 7(a), W_{LES} is extrapolated to zero at half filling for U much larger than U_c. It has a sudden increase below $U/t = 6$. This suggests that this in-gap weight won't disappear at half filling in the intermediate coupling case. Moreover, as U decreases to the weak coupling regime, as shown in the $U/t = 4$ case in Fig. 6(a), the major peak appears at the location of upper SDW states. Those upper SDW states begin to merge with the UHB and the excitation gap becomes an SDW gap and there is no clear separation between UHB and upper SDW states. This is in accordance with the mean field theory. Therefore, the disappearance of SDW states at half filling as U increases is a characteristic of Mott transition. Furthermore, we can also examine the slope of the W_{LES}. An important feature of the Mott insulator is the spectral weight of $2x + \alpha$ for the LES. In the infinite U limit, according to Ref. [36], α is proportional to $1/U$ and the slope of W_{LES} approaches but greater than 2. In this regime, as U decreases, there is an increase in the slope of W_{LES}. In the weak coupling regime, on the other hand, there is no UHB and all of the weight $1 + x$ is distributed close to the chemical potential. The transition between strong and weak coupling can be clearly seen in Fig. 7(b). As U decreases from $U/t = 16$, there is an increase in the slope of W_{LES}. As soon as U crosses the Mott transition (U_c), the slope has a sudden drop. At $U/t = 6$, the slope is much less than 2, suggesting that it has crossed U_c and Mott physics no longer applies.

IV. CONCLUSION

In summary, by using a variational approach to study the HM in the AFM phase, we construct several quasiparticle states to study the evolution of PES and, in particular, IPES, with hole doping. The substantial amount of spectral weight inside the Mott gap is due to the mostly unoccupied upper SDW bands. These states interact strongly with the UHB so that there is a large spectral weight transferred from UHB to these in-gap states. Although we use one-band HM instead of specific oxygen orbitals, we are able to capture the detail evolution of the spectrum with doping observed in the recent STS on cuprates. Our results also agree with previous numerical works with respect to the dynamical spectral-weight transfer with a renormalization of about $\alpha \sim 0.65x$ at $U/t = 10$. This agreement is a bit surprising as previous works have not included AFM order [1,35]. This may be due to the fact that for IPES, there is a much smaller incoherent spectral weight [37] and quasiparticle states we considered have almost all the spectral weights.

We would like to point out that in the lightly doped cuprate samples [21] in experiments, there is no density of states at the chemical potential. Since the sample is quite inhomogeneous, we believe that there is a strong localization effect that depletes the density of states at chemical potential. Since we have not considered the localization or disorder in our calculation, our result has a small peak near chemical potential when an electron is added to the lower SDW states. Fortunately, the in-gap states that we focused on have energy much larger than this localization gap, so that we can account for them without considering the disorder. An interesting possibility of localization may be due to the checkerboard pattern observed in [21]. In the strong coupling limit of the HM or the t-J model, it is recently shown [38] that at very low doping, there are states with checkerboard patterns involving SDW. Hence our account of SDW as the source of in-gap states may be a reasonable approximation.

One thing we want to emphasize is that the SDW gap has a much larger energy scale than the superconducting scale as well as the pseudogap scale. From our point of view, in-gap states may be found for other patterns such as pair density wave or charge density wave orders. Therefore, to look further into the pseudogap phase in the paramagnetic region, we probably need to consider inhomogeneous phases as in Ref. [38] to address these low energy scales, which is beyond our present scope and will be left for future work. Also, it is well known from other experiments and the experiment in Ref. [21] that, in the very underdoped regime, the AFM state is likely a spin glass or disordered state. Hence the superconducting phase coherence could be suppressed. In this work the disorder is not considered, so there is coexistence of superconductivity and antiferromagnetism. Nevertheless, the in-gap states we

considered here are not related to the superconducting property as the gap size is much larger than the pairing scale and its variation with U is essentially a SDW gap.

Our result also shows that the spectral distribution has a nonmonotonic behavior when U is increased above U_c to enter the Mott physics. At half filling, there is a small SDW gap at small U, and also a finite spectral weight at low energy (W_{LES}) above chemical potential. But the gap changes to the much larger Hubbard gap as U becomes larger than U_c and there is absolutely no spectral weight within the gap. After doping the energy of in-gap states changes from mean field type ($\propto U$) to t-J ($\propto 1/U$) type and leaves a peak around U_c. At small doping the low energy spectral weight above chemical potential is proportional to doping for $U > U_c$. These properties might be useful to study the Mott transition in organic superconductors [39,40], where U/t can be varied by applying pressure.

ACKNOWLEDGMENTS

We acknowledge and thank Y. Wang for helpful conversations and communications. This work was partially supported by Taiwan Ministry of Science and Technology with Grant No. 105-2112-M-001-008 and calculation was supported by the National Center for High Performance Computing in Taiwan.

[1] M. S. Hybertsen, E. B. Stechel, W. M. C. Foulkes, and M. Schlüter, Phys. Rev. B **45**, 10032 (1992).
[2] E. Dagotto, F. Ortolani, and D. Scalapino, Phys. Rev. B **46**, 3183 (1992).
[3] M. B. J. Meinders, H. Eskes, and G. A. Sawatzky, Phys. Rev. B **48**, 3916 (1993).
[4] N. Bulut, D. J. Scalapino, and S. R. White, Phys. Rev. Lett. **72**, 705 (1994).
[5] M. Jarrell, T. Maier, M. H. Hettler, and A. N. Tahvildarzadeh, Europhys. Lett. **56**, 563 (2001).
[6] H. Kajueter and G. Kotliar, Phys. Rev. Lett. **77**, 131 (1996).
[7] M. Fleck, A. I. Liechtenstein, A. M. Oleś, L. Hedin, and V. I. Anisimov, Phys. Rev. Lett. **80**, 2393 (1998).
[8] B. Kyung, S. S. Kancharla, D. Sénéchal, A.-M. S. Tremblay, M. Civelli, and G. Kotliar, Phys. Rev. B **73**, 165114 (2006).
[9] A. Liebsch, Phys. Rev. B **81**, 235133 (2010).
[10] R. Peters and N. Kawakami, Phys. Rev. B **89**, 155134 (2014).
[11] T. Ahmed, T. Das, J. J. Kas, H. Lin, B. Barbiellini, F. D. Vila, R. S. Markiewicz, A. Bansil, and J. J. Rehr, Phys. Rev. B **83**, 115117 (2011).
[12] W.-H. Leong, S.-L. Yu, T. Xiang, and J.-X. Li, Phys. Rev. B **90**, 245102 (2014).
[13] C. Ye, P. Cai, R. Yu, X. Zhou, W. Ruan, Q. Liu, C. Jin, and Y. Wang, Nat. Commun. **4**, 1365 (2013).
[14] D. Sénéchal and A.-M. S. Tremblay, Phys. Rev. Lett. **92**, 126401 (2004).
[15] D. Sénéchal, P.-L. Lavertu, M.-A. Marois, and A.-M. S. Tremblay, Phys. Rev. Lett. **94**, 156404 (2005).
[16] M. Aichhorn, E. Arrigoni, M. Potthoff, and W. Hanke, Phys. Rev. B **74**, 235117 (2006).
[17] M. Kohno, Phys. Rev. Lett. **108**, 076401 (2012).
[18] A. Krinitsyn, S. Nikolaev, and S. Ovchinnikov, J. Supercond. Novel Magn. **27**, 955 (2014).
[19] D. C. Peets, D. G. Hawthorn, K. M. Shen, Y.-J. Kim, D. S. Ellis, H. Zhang, S. Komiya, Y. Ando, G. A. Sawatzky, R. Liang, D. A. Bonn, and W. N. Hardy, Phys. Rev. Lett. **103**, 087402 (2009).
[20] Y.-J. Chen, M. G. Jiang, C. W. Luo, J.-Y. Lin, K. H. Wu, J. M. Lee, J. M. Chen, Y. K. Kuo, J. Y. Juang, and C.-Y. Mou, Phys. Rev. B **88**, 134525 (2013).
[21] P. Cai, W. Ruan, Y. Peng, C. Ye, X. Li, Z. Hao, X. Zhou, D.-H. Lee, and Y. Wang, Nat. Phys. **12**, 1047 (2016).
[22] S. Uchida, T. Ido, H. Takagi, T. Arima, Y. Tokura, and S. Tajima, Phys. Rev. B **43**, 7942 (1991).
[23] T. Katsufuji, Y. Okimoto, and Y. Tokura, Phys. Rev. Lett. **75**, 3497 (1995).
[24] W. J. Padilla, Y. S. Lee, M. Dumm, G. Blumberg, S. Ono, K. Segawa, S. Komiya, Y. Ando, and D. N. Basov, Phys. Rev. B **72**, 060511(R) (2005).
[25] V. J. Emery, Phys. Rev. Lett. **58**, 2794 (1987).
[26] J. Zaanen, G. A. Sawatzky, and J. W. Allen, Phys. Rev. Lett. **55**, 418 (1985).
[27] F. C. Zhang and T. M. Rice, Phys. Rev. B **37**, 3759 (1988).
[28] P. Horsch and W. Stephan, in *Electronic Properties of High-Tc Superconductors*, Springer Series in Solid-State Sciences Vol. 113, edited by H. Kuzmany, M. Mehring, and J. Fink (Springer, Berlin, 1993), pp. 351–367.
[29] Actually, there is still a difference between the two models when we consider charge fluctuation of doublon-hole pairs. In the one-band model there is only one kind of hole hopping processes while there are two kinds in the three-bands model. One process is simply the exchange of ZR singlet with a Cu spin as in the one-band case; the amplitude t was estimated in Ref. [27]. The other process is the formation of doublon-hole pair or Cu-$3d^{10}$-ZR singlet. This hopping amplitude is about $\bar{t} = 0.4t$.
[30] T. K. Lee and C. T. Shih, Phys. Rev. B **55**, 5983 (1997).
[31] K. Kobayashi and H. Yokoyama, Phys. Proc. **45**, 17 (2013).
[32] H. Yokoyama and H. Shiba, J. Phys. Soc. Jpn. **59**, 3669 (1990).
[33] This result overestimates the doping range for the AFM phase comparing to experiments. To be consistent with cuprate phase diagram, we need much larger U/t. This can be seen in Ref. [31], which shows that AFM disappears around $x = 0.1$ for $U/t = 30$. On the other hand, our simple wave function is not expected to produce very accurate phase diagram. To reduce the AFM phase region, we have to include more sophisticated Jastrow factor such as correlation between holes or spins on different sites, etc. Since we are only interested in the AFM state in lightly doped region, this discrepancy does not change our main conclusion.
[34] Actually, the value of ξ_0 remains the same even if we change this criterion to 0.7 or 0.9 .
[35] A. Liebsch and N.-H. Tong, Phys. Rev. B **80**, 165126 (2009).
[36] A. B. Harris and R. V. Lange, Phys. Rev. **157**, 295 (1967).
[37] M. Randeria, R. Sensarma, N. Trivedi, and F.-C. Zhang, Phys. Rev. Lett. **95**, 137001 (2005).
[38] W.-L. Tu and T.-K. Lee, Sci. Rep. **6**, 18675 (2016).
[39] S. Lefebvre, P. Wzietek, S. Brown, C. Bourbonnais, D. Jérome, C. Mézière, M. Fourmigué, and P. Batail, Phys. Rev. Lett. **85**, 5420 (2000).
[40] F. Kagawa, K. Miyagawa, and K. Kanoda, Nature (London) **436**, 534 (2005).